

# Characterization of Tribochemical Reactions on Steel Surfaces

Makoto MIYAJIMA\*  
Keishi MATSUMOTO

Kazuyuki KITAMURA

## Abstract

*Outlined herein are examples of the analysis of tribofilms forming on metal surfaces during friction under the existence of lubricating oil. Tribofilms forming on high-alloy steel surfaces through reactions of the steel and polysulfide, a sulfur-containing extreme pressure additive, were analyzed using X-ray photoelectron spectroscopy. It had different structures depending on the chemical composition of materials. The thickness of the multi-layer film was calculated through more detailed analysis. Raman spectroscopy was applied to the analysis of tribofilms of carbon steel, and the technique has proved effective at directly observing the films with lubricating oil in ambient air. Thus, it has become practicable to observe sliding surfaces during boundary lubrication in real time on a friction test device.*

## 1. Introduction

Dynamic reactions such as oxidation and corrosion take place on steel surfaces. Although less popular than these, another type of surface phenomenon is tribochemical reaction due to friction. Here friction serves as the driving force for the formation of a lubricating film called a tribofilm on the steel surface; the tribofilm suppresses or controls the friction and wear of steel. The tribochemical reaction is important especially in lubricating conditions. Since lubricant is used in many stages of steel manufacturing and applications, tribochemical reaction must always be given due consideration in the steel industry. Such tribochemical reactions take place in tightly closed spaces between solid materials, which means that the features of such reactions lag behind those of oxidation or corrosion.

To form effective tribofilms, lubricating oils contain extreme pressure (EP) additives, which are classified into chloric additives, sulfuric additives, etc. according to the component element of their functional group. EP additives are required for steel manufacturing processes such as rolling, drawing, and other plastic deforming work in cold conditions. During such cold plastic deformation, new surfaces of work pieces appear on the friction surface contacting the tools, and scuffing is likely to occur there. The EP additives used for such work are required to be highly reactive, and accordingly, active additives containing chlorine, sulfur or phosphorus have been used. However, environmental risks have been emphasized in relation to chloric additives. Some phosphoric additives adversely affect the mechanical properties of some stainless steels. Sulfur-containing additives have remained and are widely used for alloy steels.

Sulfur-containing EP additives exert excellent performance in boundary lubrication conditions and many studies have been conducted on their lubricating mechanism. As long ago as 1958, for example, Davey et al. proposed, and later Forbes et al. modified, a reaction mechanism whereby mercaptide forms under boundary lubrication with mono- or disulfide, and the mercaptide turns into sulfide.<sup>1)</sup> Mori et al. reported that iron sulfide, iron sulfate and iron oxides formed from polysulfide, which does not contain oxygen.<sup>2)</sup> Many researchers also reported that the reactions of sulfur-containing EP additives yielded sulfate and iron oxides as well as sulfide.<sup>3-5)</sup> As indicated above, any of the sulfur-containing EP additives may form various chemical compounds on steel surfaces depending on the environmental conditions. Regarding steel, many reports have dealt with the reactions of sulfur-containing EP additives with pure iron or carbon steel. The most important consideration for switching to Cl-free lubricant is understanding the lubricating mechanism between EP additives and high alloy steels containing much Cr and Ni, but there have been very few reports on this aspect.<sup>6)</sup>

With respect to the analytical techniques of tribofilms, electron probe micro analysis (EPMA) and Auger electron spectroscopy (AES) are employed for element analysis. X-ray photoelectron spectroscopy (XPS), secondary ion mass spectrometry (SIMS), Raman spectroscopy and Fourier transform infrared spectroscopy (FT-IR) are employed for structural analysis; they are used in combination with each other as required.<sup>7-11)</sup>

XPS is excellent in element analysis in terms of quantitative accuracy and in the chemical state analysis in terms of compound

\* Researcher, Fundamental Metallurgy Research Lab., Advanced Technology Research Laboratories  
1-8 Fuso-cho, Amagasaki, Hyogo Pref. 660-0891

identification. It has long been used for analysis of the chemical state of friction surfaces, and is still the most widely used technique for such purpose. However, most surface analytical techniques such as XPS must be performed in a vacuum in order to use electron beams. They cannot directly analyze friction surfaces with a lubricating oil. While the state of a surface during friction is considered different from that post friction, XPS can deal with the state after friction. There is no telling whether oxide detected in the analysis is formed during the friction or during atmospheric exposure post friction, which has often caused dispute.

FT-IR and Raman spectroscopy are able to perform in ambient air to use light for detection. In situ observation techniques on the friction surfaces using FT-IR are practically available. These have actually been employed for analyzing the change in the concentration of organic compounds in lubricating oil on friction surfaces.<sup>12)</sup> Focusing on the analysis of tribofilms of inorganic compounds, Raman spectroscopy is better than FT-IR. It has been used for in situ observation of lubricant: one such report describes the process by which  $\text{MoS}_2$  in a solid lubricant turned into  $\text{MoS}_3$ .<sup>13)</sup> However, there have been few reports of in situ observation of tribofilms forming through reactions of EP additives using Raman spectroscopy.

In this study, we conducted friction tests of a sulfur-containing EP additive on Fe-Cr-Ni steels and other metal materials, and through analysis of the structure of the tribofilms thus formed using XPS, examined the mechanisms of the tribochemical reactions. The possibility of in situ observation of tribofilms with lubricating oil was investigated using Raman spectroscopy.

## 2. Test Method

### 2.1 Friction test

We conducted a friction test under lubrication using a ball-on-disk tribometer schematically shown in **Fig. 1**. We investigated the change in the friction coefficient under boundary lubrication. The test condition was as follows: the entire friction surfaces were covered with lubricant; the load was 10 N (maximum Hertz pressure was 1.4 GPa); the friction speed was 0.01 m/s; the total friction distance was 12 m; and the test temperature was 100°C. A 6.35 mm diameter SUJ2 ball, which was equivalent to AISI 52100, was used as the pin. The following materials were used for the disk: carbon steel (C/S); 18Cr8Ni stainless steel (S/S); 25Cr35Ni high-alloy steel (H/A); 16Cr73Ni alloy (Ni/A); pure nickel (Ni); and pure chromium (Cr). The test surface of these specimen disks, 3 mm in thickness and 20 mm in diameter, was mirror-polished to  $R_a=0.01 \mu\text{m}$  by buffing. **Table 1** shows the chemical compositions of the disks. Polysulfide (di (tert-dodecyl) penta-sulfide,  $\text{C}_{12}\text{H}_{25}\text{-S}_5\text{-C}_{12}\text{H}_{25}$ ), a typical sulfur-containing EP additive, was used without dilution for the lubricant.

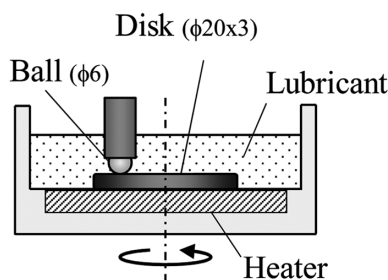


**Fig. 1** Schematic illustration of ball-on-disk tribometer

**Table 1** Chemical compositions of the disk materials

	C	Si	Mn	P	S	Ni	Cr	Fe
(1) C/S	0.45	0.23	0.83	0.02	0.01	0.01	0.12	Bal.
(2) S/S	0.50	0.54	1.50	0.02	0.01	9.50	18.5	Bal.
(3) H/A	0.03	0.40	0.60	0.02		35.0	25.0	Bal.
(4) Ni/A	0.03	0.20	0.19			72.1	15.9	Bal.
(5) Ni			0.11			>99.8		
(6) Cr							>99.9	

(Mass %)

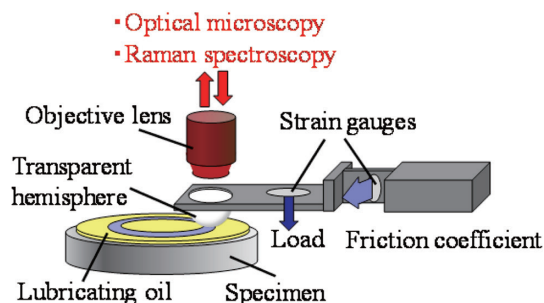


**Fig. 2** Schematic illustration of in situ Raman tribometer<sup>15)</sup>

### 2.2 XPS analysis

After the test, the disks were cleaned of residual additive by ultrasonic cleaning in a bath of a polar organic solvent (ethyl methyl ketone) and another of a nonpolar organic solvent (cyclohexane). Then, the disk surface was analyzed using XPS. A monochromated  $\text{Al K}\alpha$  (1486.6 eV) beam was irradiated at a pass energy of 55.0 eV and in a diameter of  $40 \mu\text{m}$ ; no charge-neutralizing electron gun was used. The chemical state on the surface was specified, and in addition, the thickness of the tribofilm was estimated assuming that it consisted of multiple layers. More specifically, an organic layer and an oxide layer were assumed to be on the base metal surface (three layers in total) as proposed by Asami et al., and their chemical compositions and thicknesses were estimated using a non-destructive quantitative analysis method<sup>14)</sup> based on the curve-fitting data of XPS.

### 2.3 Raman spectroscopy analysis

Tribofilms formed from the polysulfide on the carbon steel (C/S) were examined using ex situ Raman spectroscopy to investigate the possibility of in situ observation of the tribofilm formation process. A spatial resolution roughly  $2 \mu\text{m}$  in diameter was obtained by using a visible light 532 nm in excitation wavelength emitted from a solid laser and a  $50\times$  objective lens. The friction surfaces were analyzed either after degreasing with acetone or without cleaning. In addition, in situ observation was performed for investigating real friction phenomena using the device illustrated in **Fig. 2**<sup>15)</sup>. While an SUJ2 ball was used for the tester given in **Fig. 1**, this device used a  $\text{SiO}_2$  transparent hemispherical lens to directly observe the contact interface.

## 3. Test Results

### 3.1 Observation of friction surfaces

**Figure 3**<sup>16)</sup> shows optical micrographs of the surfaces of the disks and balls after the ball-on-disk tribotest. The disks contained the following: friction scratches were seen with the C/S disk, and in addition, there were color-changed spots resembling corrosion pits resulting from the formation of tribofilms; friction scratches were

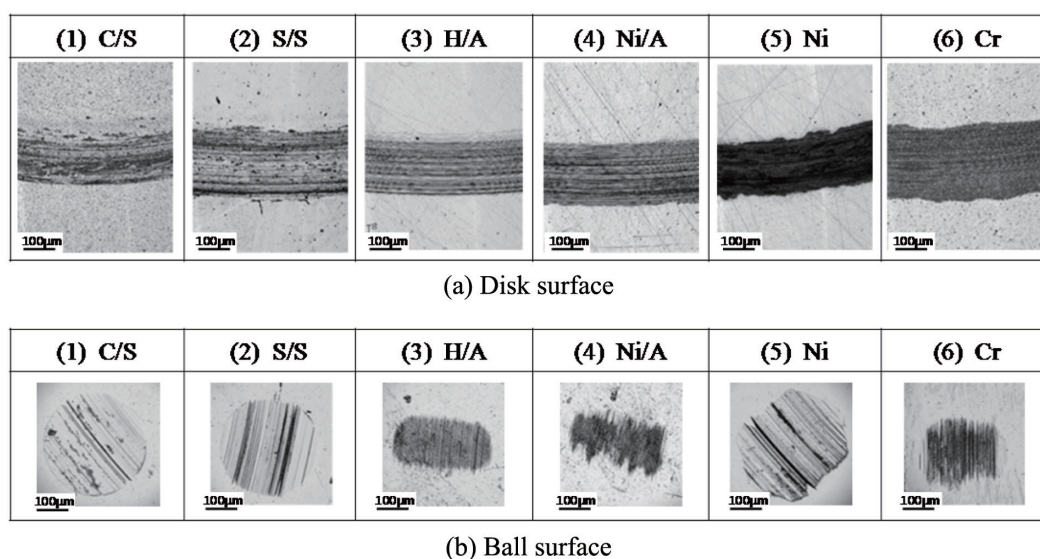


Fig. 3 Optical micrographs of disk and ball surfaces after tribo-test<sup>16)</sup>

found with the S/S, H/A and Ni/A disks in increasing degrees in this order, while slight color change due to the tribochemical reaction between the metal and the additive was seen on their entire friction surfaces in decreasing degrees; none of the Ni and Cr disks had conspicuous friction marks, but the entire friction surfaces changed color significantly. As described above, color change due to the reaction was seen with the Ni/A, Ni and Cr disks, which indicates that tribofilms formed on their surfaces.

The surfaces of the balls that contacted the disks contained the following: the one for the C/S disk had slight friction marks on the entire surface area, and there were partially pit-like color-changed spots probably resulting from the reactions between the ball material and the additive; that for the S/S disk had conspicuous friction scratches on the surface but there were no color-changed spots; the balls for the H/A and the Ni/A disks had distinct scratches, some were extremely deep, which indicates that the friction was considerably severe; likewise, those for the Ni and Cr disks had deep scratches. From the above observation results of the disks and balls, the friction was presumed to be comparatively mild with the C/S and the S/S disks, but in contrast, it was increasingly severe with the H/A, the Ni/A, the Ni and the Cr disks, in this order.

### 3.2 XPS analysis

Figure 4<sup>16)</sup> shows the spectra of the frictional and non-frictional areas of the disks obtained through the XPS analysis. The curves were obtained by subtracting the background from raw spectra by Shirley's method, curve fitting, and then correcting them assuming that the binding energy of a -C-C- coupling in C 1s was 285.0 eV. The ordinates of the graphs are in arbitrary units, and the peak intensities of all the spectra are reduced to the same height.

The frictional areas revealed the following. There was mainly FeS<sub>2</sub> on the C/S disk. The oxides described later and a small amount of FeS were found on the S/S disk. In consideration of the position of the peak of Fe2p<sub>3/2</sub>, the peak of S2p<sub>3/2</sub> near 162.8 eV was not attributed to FeS<sub>2</sub>; judging from its position, it may possibly be of Fe-containing mercaptide.<sup>4)</sup> FeS and NiS<sub>2</sub> were found on the H/A disk. NiS<sub>2</sub> was mainly found on the Ni/A disk, and NiS and Cr<sub>2</sub>S<sub>3</sub> were found on the Ni and the Cr disks, respectively. In addition, a small amount of sulfates was found on all the disks. Cu-sulfides were found on the Ni and Cr disks, originating from inevitable im-

purity Cu. There were oxides on every disk judging from the spectra of O1s. There were iron oxides and hydroxides peaks on the C/S disk, and there were iron oxide peaks and another near 531.8 eV, assumed to be of Cr oxide or Fe hydroxide on the S/S and the H/A disks.

A peak identified to be that of Ni hydroxide was found on the Ni and the Ni/A disks, and there was a slight peak of Fe hydroxide found on the Ni/A disk. Cr<sub>2</sub>O<sub>3</sub> was found on the Cr disk. While the fact that oxides are found on the friction surfaces agrees with the past study results on Fe samples described earlier,<sup>3-5)</sup> oxides were found also on Fe-Cr-Ni, Cr and Ni disks in the present test. This means that oxides were also mixed together with sulfide films resulting from the tribochemical reactions on Fe-Cr-Ni alloys. On the other hand, very small amounts of sulfates and no sulfides were found in the non-frictional areas of all disks. In addition, no sulfur compounds whatsoever were found in the non-frictional areas of the Cr or Ni disks. The same oxides were found in the frictional and the non-frictional areas.

To determine in what state the oxides and the reaction products (sulfides) coexisted on the friction surfaces, we obtained the mapping images of the C/S, the S/S and the Ni/A disks. Figure 5<sup>16)</sup> shows the secondary electron images, the mapping images in the sulfide range (158 to 164 eV), the same in the sulfate range (164 to 172 eV) of S2p of XPS, and those in the range of oxide and hydroxide (529 to 531.5 eV) of O1s. These mapping images were taken across boundaries between the frictional and the non-frictional areas, the former being on the lower right side of each frame, and the latter on the upper left. Much sulfide was detected in the frictional areas of the C/S and the Ni/A disks. Similarly, more sulfide was found in the frictional area of the S/S disk than in the non-frictional area.

In contrast, low intensities of sulfate were detected. There was little difference between the two areas of these specimens. In the oxide mappings of O1s, the intensity was substantially even in all the frames, indicating that oxide was distributed homogeneously. From the fact that sulfide and oxide are distributed evenly in the entire frictional area, they exist in the form either of finely mixed single layer or of two separate layers. However, as described later in relation to the quantitative analysis, they are presumed to exist in

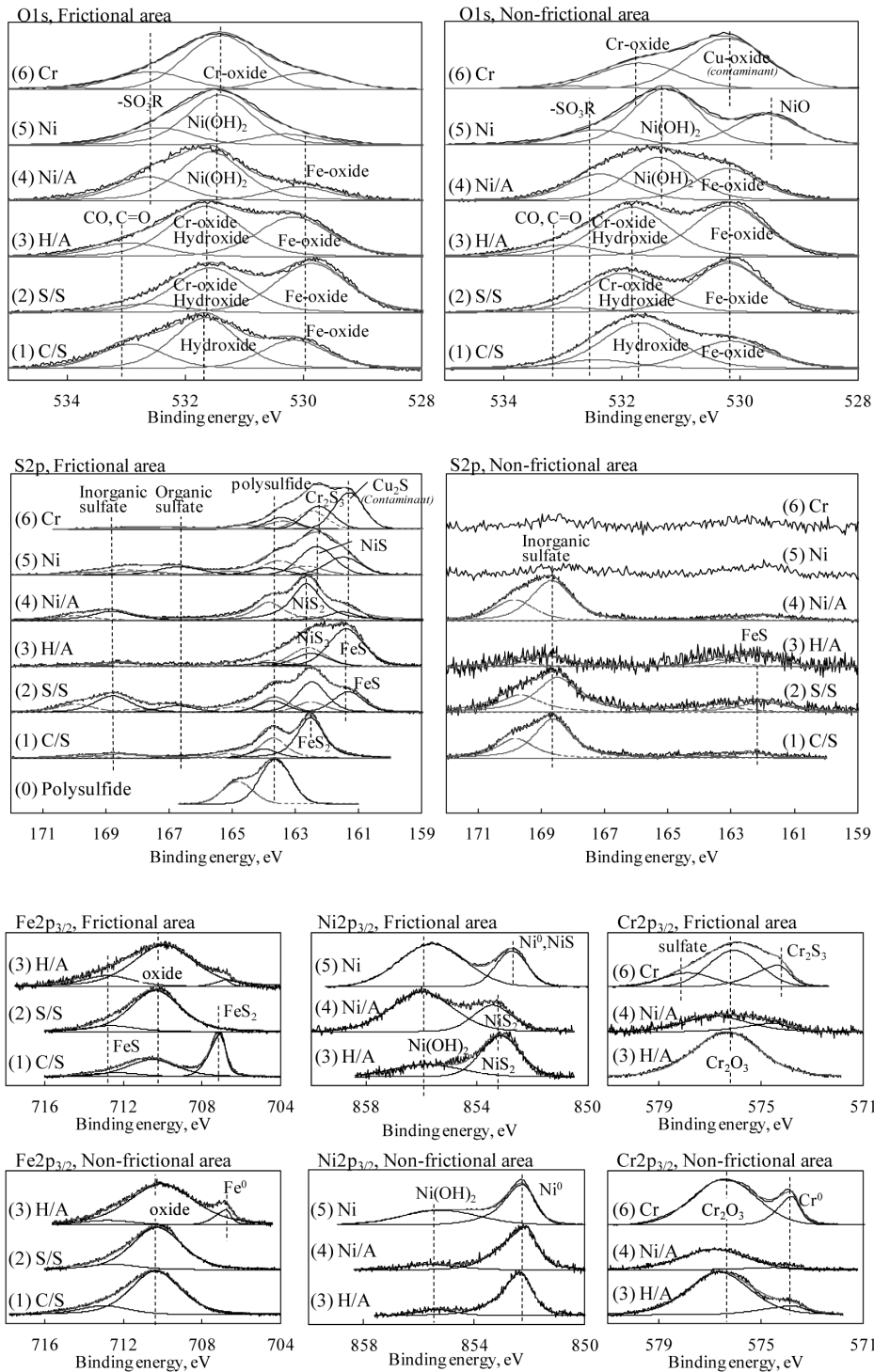


Fig. 4 Small-area XPS analysis in frictional and non-frictional areas of disks after tribo-test<sup>16)</sup>

two layers, sulfide over oxide. It must be noted here that the XPS mappings were made by scanning the field using an analysis beam roughly 40 μm in diameter. As a result, the spatial resolution is not as good as the dots of the images suggest.

Figure 6<sup>16)</sup> schematically shows the structures of tribofilms originating from polysulfide presumed from the above. Oxide exists in both the frictional and the non-frictional areas of all disks. A layer of Fe sulfide forms on the oxide layer in the frictional area of the C/S

and the S/S disks. That of Ni sulfide forms on the oxide layer in the frictional area of the Ni/A and the Ni disks. That of Cr<sub>2</sub>S<sub>3</sub> forms on the oxide layer in the frictional area of the Cr disk. The Fe sulfide layers consist of FeS<sub>2</sub> and FeS on the C/S and S/S disks, respectively. The Ni sulfide layers consist of NiS<sub>2</sub> and NiS on the Ni/A and Ni disk, respectively. This is presumably due to the difference in the ease of sulfurizing, or the difference in the resistance to sulfuric corrosion, between the materials.

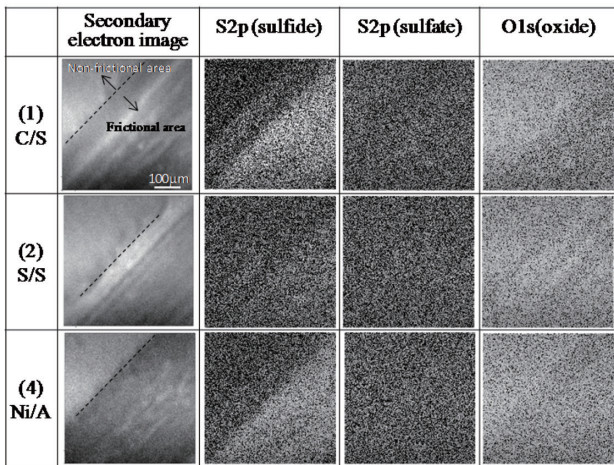


Fig. 5 XPS mapping images of disk surfaces after tribo-test<sup>16)</sup>

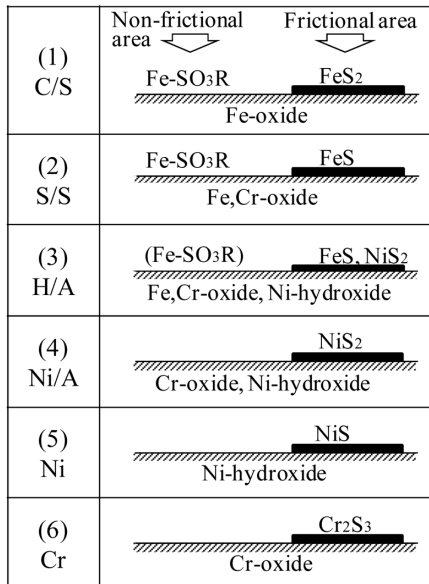


Fig. 6 Schematic diagrams of tribofilm structure on disk surfaces after tribo-test<sup>16)</sup>

Although the present test result indicates that the oxide layer is beneath the sulfide layer, it does not necessarily mean that the sulfide results from reactions between oxide and the polysulfide. For example, sulfurizing and oxidizing may occur in parallel on a newly exposed surface of Fe or Ni, but this remains uncertain since the test was not conducted in a perfectly inert atmosphere. In contrast, Fe sulfate forms in the C/S and the S/S disks, and Ni sulfate in the Ni/A disk in the non-frictional areas. It is possible that oxygen atoms in the oxide do not detach from it, and yet react with S atoms. Neither a reaction film nor an adsorption film forms in the non-frictional areas of the Cr and the Ni disks.

Regarding the disk surfaces after the friction test using the additive, a three-layer model is assumed<sup>14)</sup> as shown in Fig. 7<sup>16)</sup>, comprising the base metal, the middle layer of an oxide film and the top layer of a reaction film. The thicknesses of the layers were estimated quantitatively from the peak intensity of the photoelectron spectrum of each compound, assuming that each of the layers is of a homogeneous structure and that no mutual dispersion occurs between the

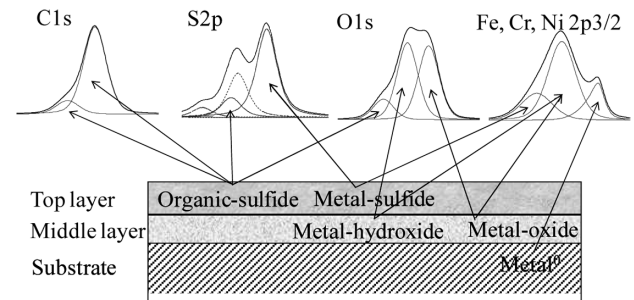


Fig. 7 Schematic description of quantitative analysis method using three-layer model<sup>16)</sup>

layers. Here, the relationship between the photoelectron spectrum intensity and the structure and thickness of the films can be expressed in the form of the following equations (1) to (3),

$$I_i^m = (g_i \sigma_i^m C_i \rho^m \Lambda_i^m / A_i) \cdot \exp(-t/\Lambda_i^{ox}) \cdot \exp(-l/\Lambda_i^{con}) \quad (1)$$

$$I_j^{ox} = (g_j \sigma_j^{ox} C_j \rho^{ox} \Lambda_j^{ox} / A_j) \cdot [1 - \exp(-t/\Lambda_j^{ox})] \cdot \exp(-l/\Lambda_j^{con}) \quad (2)$$

$$I_k^{con} = (g_k \sigma_k^{con} C_k \rho^{con} \Lambda_k^{con} / A_k) \cdot [1 - \exp(-l/\Lambda_k^{con})] \quad (3)$$

Here, upper suffixes *m*, *ox*, and *con* stand for the base metal, the middle (oxide) layer and the top (contamination) layer, respectively; and lower suffixes *i*, *j* and *k* for elements, respectively, of the base metal, the middle layer and the top layer; *I* is integrated peak intensity; *g* is the geometrical factor;  $\sigma$  is the photoionization sectional area;  $\Lambda$  is the effective escape depth of photoelectron;  $\rho$  is density; *A* is atomic weight; *t* is the thickness of the middle layer; and *l* is the same of the top layer. The layer thicknesses are given by substituting the curve-fitting data of the XPS obtained in the above equations and solving them simultaneously. The parameter values were set referring to the literature of Asami et al.<sup>14)</sup> and Elsener et al.<sup>17)</sup>, and from the values of *t* and *l* thus obtained, the mass fraction *C* of each layer was calculated.

Figure 8<sup>16)</sup> shows the thicknesses and compositions of the top and the oxide layers of the three-layer model for both the frictional and the non-frictional areas. With respect to the top layer given in part (a), it is thicker in the frictional area than in the non-frictional area with all the disks. Although tribofilm is formed in the frictional area through tribochemical reactions, the top layer is not very thick under the conditions of the present test, probably because it is continuously ground off by the friction. The top layer thicknesses of the high-alloy disks (H/A, Ni/A, etc.) are no different from those of the Fe-base disks such as C/S and S/S, which means that high-alloy steels are not necessarily more resistant to tribochemical reactions. The compositions of the films in the non-frictional area consist mostly of organic compounds. Small amounts of sulfate compounds were found in the non-frictional area of C/S and the S/S disks.

Fe sulfide formed beneath the layer of adsorbed organics in the frictional area of the Fe-base disks. Ni sulfide formed in the frictional area of high-alloy steels. Cr sulfide formed in the frictional area of the Cr disk. Ni sulfide formed in the frictional area of the Fe-Cr-Ni disk, but Cr sulfide did not.

With respect to the middle (oxide) layer given in part (b) of Fig. 8, those of the H/A and the Ni/A disks were slightly thicker in the frictional area than in the non-frictional area. We thought initially that oxide in the frictional area would be worn off by the friction, and the layer thinner, but the actual finding was to the contrary. Since the test was conducted in an oil bath, the molecules of which do not contain oxygen atoms, the only possible reason for the thicker oxide layer is either that the material was oxidized during

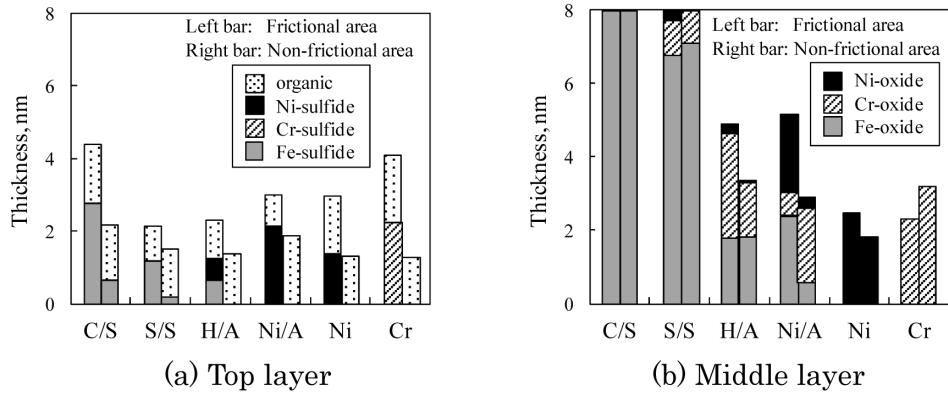


Fig. 8 Thicknesses and compositions of top and oxide layers after tribo-test<sup>16)</sup>

friction by oxygen solute in the oil or that oxidation occurred in the atmosphere during washing and other treatment after the test. If the latter is the case, however, it cannot explain the oxidation in priority in the frictional area, and therefore we believe oxidation must have occurred during the friction. The chemical composition of the oxide layer reflected that of each specimen disk: the middle layers of the C/S and the S/S disks consisted of iron oxide; those of the H/A and the Ni/A disks consisted of Cr oxide, Ni oxide and their hydroxides in ratios according to the contents of the respective elements.

3.3 Raman spectroscopy analysis

To confirm the applicability of Raman spectroscopy to the analysis of the tribofilms of the C/S disk, a test analysis was conducted ex situ. Figure 9<sup>18)</sup> shows the Raman spectra of the surface of a C/S disk after a friction test at 200°C for 20 min and cleaning with acetone thereafter. Peaks of iron sulfide ( $FeS_2$ ) were found at 339 and 373  $cm^{-1}$  on the friction mark (curve (a)), which agrees with the XPS results given in Figs. 4 and 6. Curve (a) also has two gentle peaks in the range of 1300 to 1600  $cm^{-1}$ ; they proved to be the D and the G bands due to graphite structure. They appeared presumably through the following mechanisms: when a tribofilm of  $FeS_2$  forms, the S-S coupling in polysulfide breaks and the hydrocarbon radical decomposes, forming structures leading to the D and the G bands.

Although it is possible to detect organic compounds on the surface using C1s peaks of XPS as shown in Fig. 7, it is impossible to specify their structure, but it was a significant finding that Raman spectroscopy can detect the components of tribofilms other than sulfide. The  $FeS_2$  peaks were also found in area (b) of Fig. 9, where the tribofilm looks to have flaked off, inside a friction mark, although the peak intensity was less than 1/20 of that in area (a). It is assumed that a tribofilm grows quickly to be thick enough to flake off easily at 200°C. For comparison, curve (c) of Fig. 9 is the spectrum of the mirror-polished disk surface before the friction test: there was only a very low peak near 660  $cm^{-1}$  attributed to  $Fe_3O_4$ .

As an approach to in situ observation, friction marks were examined using Raman spectroscopy without cleaning the oil as shown in Fig. 10<sup>18)</sup>. After a 1 min friction test at 200°C with polysulfide,  $FeS_2$  peaks were seen, while many peaks attributable to polysulfide were seen in the range from 200 to 1800  $cm^{-1}$ . Another specimen was analyzed after a 20 min test in a mineral oil at room temperature (25°C), and while several peaks were identified as being from the mineral oil, a peak attributable to  $Fe_3O_4$  was distinctly confirmed.  $Fe_3O_4$  existed at a friction mark in mineral oil which does not include oxygen atoms. This seems to indicate that oxygen in the

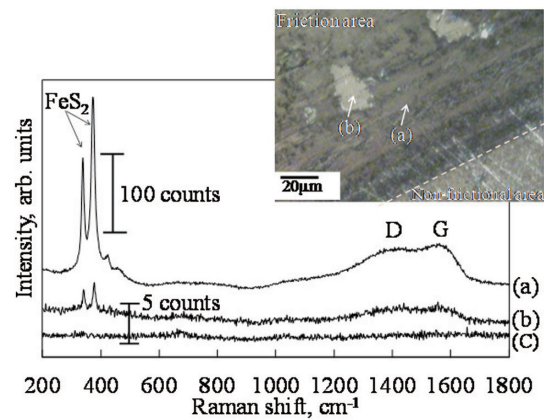


Fig. 9 Raman spectra of frictional area after acetone cleaning (a) tribofilm, (b) tribofilm flaked off, (c) before test (mirror-polished)<sup>18)</sup>

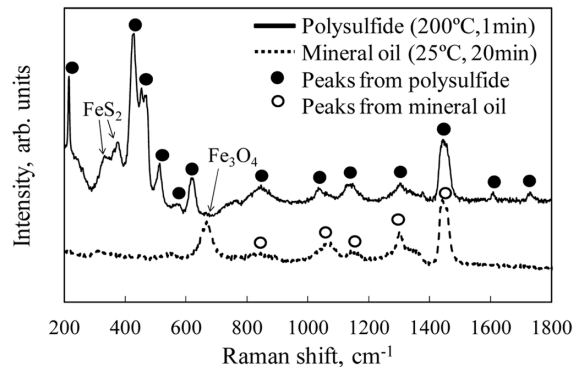


Fig. 10 Raman spectra on friction track covered with polysulfide (200°C, 1 min) and with mineral oil (25°C, 20 min)<sup>18)</sup>

atmosphere was taken into the oil by the friction or that there was oxygen solute in the oil, and such oxygen reacted with the metal on the disk surface. Thus, Raman scattering spectroscopy has proved capable of identifying  $FeS_2$  and  $Fe_3O_4$  in a tribofilm through a lubricating oil.

However, depending on test conditions (temperature, duration, etc.), there were cases where peaks were hidden by the background from degraded lubricating oil and could not be detected.<sup>19)</sup> It has also become clear that Raman spectroscopy is not applicable when the peaks of the tribofilm and those of the lubricant coincide with

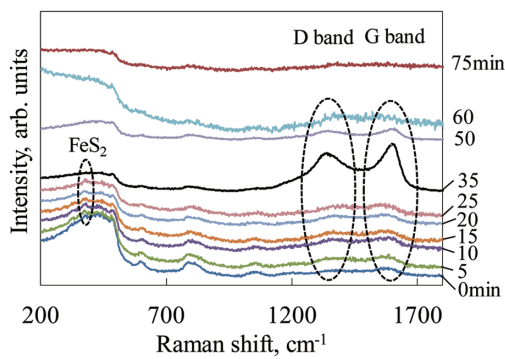


Fig. 11 Raman spectra at friction processes from lubrication to scuffing<sup>19, 20)</sup>

each other.

### 3.4 In situ observation of tribofilms using Raman spectroscopy

As seen with Fig. 10, it was possible to examine the structure of tribofilms and iron oxide through lubricating oil. Based on this, we conducted in situ observation of friction interfaces using the equipment given in Fig. 2. **Figure 11**<sup>19, 20)</sup> shows the results of the in situ observation of friction processes during the process from lubrication through oil depletion down to scuffing. In the test, which was conducted at 150°C, a FeS<sub>2</sub> tribofilm formed on the friction surface at an early stage (0 to 25 min), then the intensity of the D and the G bands increased (35 min), and scuffing occurred finally.<sup>19, 20)</sup> Although the lubricant was substantially depleted immediately before the scuffing, there was a situation where a tribofilm maintained its lubricating effects and scuffing was prevented from occurring.<sup>15)</sup>

## 4. Conclusions

Tribofilms forming on friction surfaces of various alloy steels were analyzed using XPS, and had widely different structures and thicknesses. In addition, Raman spectroscopy has proved capable of directly observing tribofilms in lubricating oil and thus capturing their structural change dynamically.

There is no such thing as an all-purpose technique for surface

analysis; to analyze the structure and the forming mechanisms of tribofilms, therefore, different analysis techniques must be used in combination. Existing analytical techniques are insufficient for clarifying the phenomena occurring on friction surfaces, and new techniques specialized in tribology are required. Many academic and research institutes conduct studies to devise unique test facilities and analytical techniques according to their objectives. Our aim is to further enhance steel-surface functions through the improvement of analysis technology.

## References

- 1) Davey, W., Edwards, E. D.: *Wear*. 1 (4), 291 (1958)
- 2) Mori, M., Hori, K., Tamai, Y.: *J. Japan Soc. Lub. Engrs.* 27 (2), 505 (1982)
- 3) Toyoguchi, M., Takai, Y.: *Bull. ASLE Transactions*. 5 (1), 57 (1962)
- 4) Bird, R. J., Galvin, G. D.: *Wear*. 37 (1), 143 (1976)
- 5) Tomura, M., Hironaka, S., Sakurai, T.: *Wear*. 41 (1), 117 (1977)
- 6) Petrushina, I. M., Christensen, E., Bergqvist, R. S., Møller, P. B., Bjerrum, N. J., Høj, J., Kann, G., Chorkendorff, I.: *Wear*. 246 (1–2), 98 (2000)
- 7) Cao, L., Sun, Y. M., Zheng, L. Q.: *Wear*. 140 (2), 345 (1990)
- 8) Choi, J., Ishii, K., Kato, T., Kawaguchi, M.: *Tribologist*. 58 (8), 596 (2013)
- 9) Kubo, T., Nanao, H., Minami, I., Mori, M., Ichihashi, T.: *Tribologist*. 51 (11), 819 (2006)
- 10) Uchidate, M., Iwabuchi, A., Liu, S., Shimizu, T.: *Tribologist*. 49 (2), 181 (2004)
- 11) Piras, F. M., Rossi, A., Spencer, N. D.: *Tribology Letters*. 15 (3), 181 (2003)
- 12) Ichihashi, T., Kudo, M., Mori, M.: *Tribologist*. 58 (8), 581 (2013)
- 13) Muratore, C., Bultman, J. E., Aouadi, S. M., Voevodin, A. A.: *Wear*. 270, 140 (2011)
- 14) Asami, K., Hashimoto, K., Shimodaira, S.: *Corros. Sci.* 17 (9), 713 (1977)
- 15) Miyajima, M., Kitamura, K., Matsumoto, K.: *Tribology Conference 2014 Autumn Morioka*. Nov. 2014, E28
- 16) Matsumoto, K., Miyajima, M., Kitamura, K.: *Tribologist*. 59 (10), 636 (2014)
- 17) Elsener, B., Rossi, A.: *Material Science Forum*. 192, 225 (1995)
- 18) Miyajima, M., Kitamura, K., Matsumoto, K.: *Tribologist*. 59 (11), 724 (2014)
- 19) Miyajima, M., Kitamura, K., Matsumoto, K.: *Tribology Conference 2014 Spring Tokyo*. May 2014, C22
- 20) Miyajima, M., Kitamura, K., Matsumoto, K.: *J. JSAE*. 69 (10), 87 (2015)



Makoto MIYAJIMA  
Researcher  
Fundamental Metallurgy Research Lab.  
Advanced Technology Research Laboratories  
1-8 Fuso-cho, Amagasaki, Hyogo Pref. 660-0891



Keishi MATSUMOTO  
Senior Researcher, Ph. D  
Fundamental Metallurgy Research Lab.  
Advanced Technology Research Laboratories



Kazuyuki KITAMURA  
Senior Researcher  
Fundamental Metallurgy Research Lab.  
Advanced Technology Research Laboratories